International Conference on Fast Sea Transportation
FAST'2005, June 2005, St.Petersburg, Russia

ON THE ADDED RESISTANCE OF CATAMARANS IN WAVES

Tony Armstrong and Anton Schmieman
Austal Ships
100, Clarence Beach Road, Henderson, Australia

ABSTRACT

The resistance of two types of catamaran hull form are determined from model test experiments in regular waves at a variety of ship speeds and headings. These are compared with each other, and a method proposed to predict the added resistance at any heading. A simple numerical prediction method is described, based upon motion transfer functions, and is compared with the experimental results. A worked example is given, together with numerical data to allow for the estimation of the necessary damping coefficients.

INTRODUCTION

Contracts for the construction of high-speed craft usually contain requirements for the speed that has to be achieved on trials in calm water. However, operators of such craft usually have to run their craft in waves, and this reduces the achievable speed. The operator may be disappointed to find that they cannot operate the craft at the trial speed. Previously there has been no known information available on the speed loss associated with the operation of catamarans in waves, and it was for this reason that the current research was undertaken.

1. EXPERIMENTATION

1.1. Hull Forms

Modern high-speed catamarans generally fall into two broad hull shape categories, depending upon the intended design speed;

Round bilge	$Fn \leq 1.0$
Hard chine form	$Fn \geq 1.0$

Two such forms were identified, suitable for use as a passenger ferry with a waterline length L of 65 m.

	Symbol	Hard chine	Round bilge
Length WL	L	65.0 m	65.0 m
Beam demihull	b	3.51 m	5.58 m
Draught	T	2.04 m	2.40 m
Displacement	Δ	713 t	779 t
Hull separation	S_H	11.8 m	13.5 m
Pitch R.O.G.	k_{yy}	20.7 m	18.3 m
Speed	V	50 kn	35 kn
Froude number	Fn	1.01	0.71

Table 1: *Particulars of the two designs*

The main particulars are given in Table 1, and the hull forms are illustrated in Figures 1(a) and 1(b). The round bilge hull form is of the semi-SWATH type, having a bulbous forward end to minimise resistance and pitching motion. The bilge radius reduces to a small value at the transom.

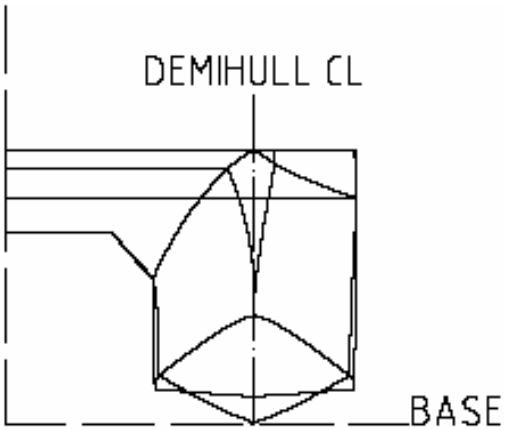

Figure 1(a): *Hard chine hull form*

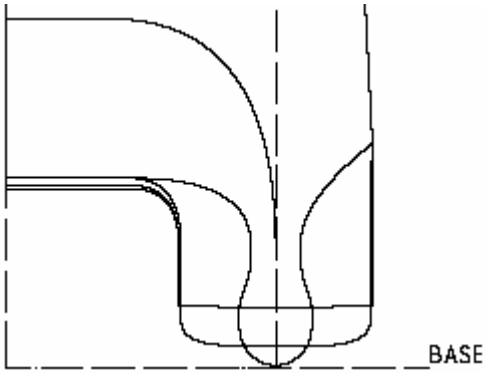

Figure 1(b): *Round bilge hull form, of semi-SWATH type*

1.2 Experimental set-up

A model of each hull form was manufactured as a catamaran with a length of 2.19 m, and tested in the 60 m towing tank at the Australian Maritime College. This is quite a small facility, and the models are restricted in size because of the maximum carriage speed and tank length, however it has previously been our experience that this is much less important for long slender hull forms with transom sterns such as those used for high speed catamarans, and close correlation has been found with the results from much larger models tested at establishments with much longer tanks. Therefore it is believed that the results are not affected by the apparently small scale of the models.

Measurements of the resistance were taken in calm water at a variety of speeds. Turbulence stimulation was applied to these models. Care was taken to model the correct pitch radius of gyration.

Measurements were then taken of resistance, heave and pitch, at three ship speeds, 15, 25 and 35 knots, in regular waves, in head seas and following seas. The wave amplitude was equivalent to 1.0 m at full scale.

1.3. Experimental Results

The typical method of expressing Added Resistance is as a non-dimensionalised value σ_{AW} based upon water density ρ, wave amplitude ζ_a and the length L and beam b on the waterline of one demihull:

$$\sigma_{AW} = \frac{R_{AW}}{\rho \zeta_a{}^2 (b^2 / L)} \qquad (1)$$

The non-dimensional added resistance values from the model tests are illustrated in Figures 2(a) to 2(c) for head seas, and Figures 2(d) to 2(f) for following seas.

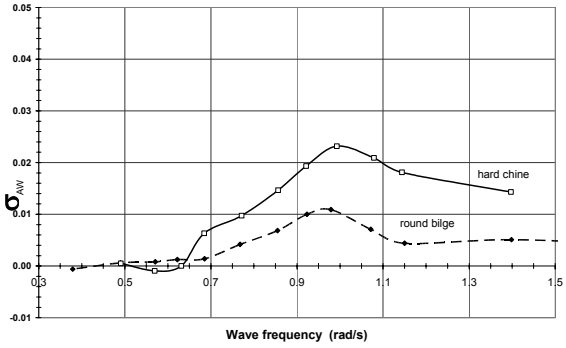

Figure 2(a): *Head sea RAOs at 13.8 knots*

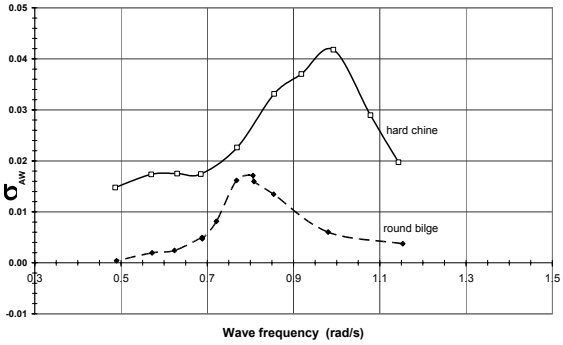

Figure 2(b): *Head sea RAOs at 23 knots*

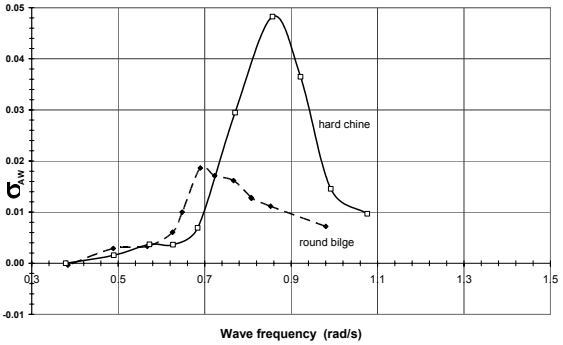

Figure 2(c): *Head sea RAOs at 32.2 knots*

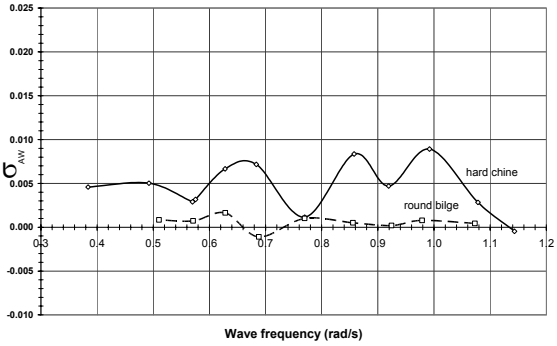

Figure 2(d): *Following sea RAOs at 13.8 knots*

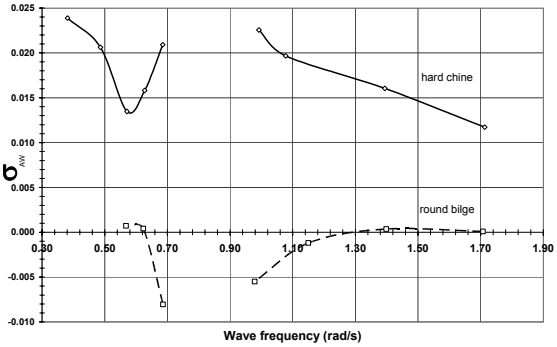

Figure 2(e): *Following sea RAOs at 23 knots*

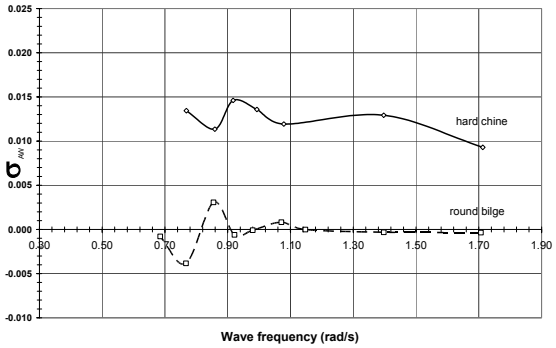

Figure 2(f): *Following sea RAOs at 32.2 knots*

The additional resistance in waves can clearly be seen to be substantially greater for the hard chine hull form compared with the round bilge hull form at almost all frequencies and at all speeds, in both head seas and following seas.

It might be anticipated that the peak of added resistance might occur at some constant value of encounter frequency. This is true for the round bilge hull form, and the peak occurs at an encounter frequency of about 9 rad/s at all ship speeds, as illustrated in Figure 3. This is the same encounter frequency as the peak in the Heave motion, but well above the encounter frequency which represents the peak in the Pitch motion. This suggests that added resistance is affected by heave more than pitch for the round bilge hull form. For the hard chine hull form, the encounter frequency of the peak of added resistance varies from a value of about 9.0 rad/s at 13.8 knots up to a value of about 12 rad/s at 32.2 kn. It appears that the hard chine hull form might have a double peak which coincides with the peaks of the heave and pitch motions, and both may drive the added resistance of this hull form. It should also be noted that the round bilge hull form has a much greater beam than the hard chine hull, and this may also have some influence. It is considered as surprising by the author that the added resistance of the wider hull is less than that of the narrow hull.

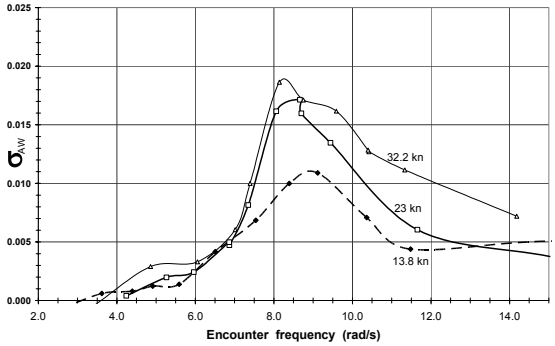

Figure 3*: Added resistance for the round bilge hull form at varying speed, illustrating similarity of peak frequency*

In following seas the round bilge hull form exhibits almost zero added resistance; the hard chine hull form demonstrates much greater values. However the accuracy of the results illustrated in Figures 2(d) to 2(f) is affected by the limited length of the towing tank, which severely restricts the number of wave encounters that can be achieved in one run. To achieve better accuracy it would be necessary to do many more runs in the same wave environment, or to utilize a longer towing tank.

It is difficult to conduct tests in following seas, particularly when the ship speed is close to the wave speed. In this case the location of the model on the wave at the commencement of the test becomes the determining factor of the magnitude of added resistance. It is for this reason that no results are presented at wave frequencies between 0.7 rad/s and 1.0 rad/s in Figure 2(e).

1.5. Transfer to irregular seas spectrum

The non-dimensional values of added resistance at various wave frequencies can be treated as Response Amplitude Operators (RAOs) and used to obtain the vessel added resistance in irregular seas in a similar fashion to the prediction of ship motions in irregular seas, by the linear superposition technique.

Knowing the wave spectrum for the sea area of interest, or from a standard spectrum such as the JONSWAP or ITTC spectrum, the ordinate of the encountered sea spectrum can be obtained. The product of this value and that of the added resistance RAO for the same encountered wave frequency gives the ordinate of the response spectrum. Summing up the response spectrum gives the mean added resistance for that irregular sea. Note that the rms value of the area of the response spectrum is twice the area of the response spectrum.

Mean added resistance is

$$R_{AW} = 2\int_0^\infty S_\zeta(\omega_e)\frac{R_{AW}}{\zeta_a^2}(\omega_e)d\omega_e \qquad (2)$$

The exact method used to transfer the results from regular seas to an irregular sea spectrum is covered by a number of texts, such as Lamb(5), Lloyd (6) and Bhattacharyya (3)

2. NUMERICAL SIMULATION

2.1. Approach

Joosen (1) derived an expression (3) by evaluating the work done by the waves and the work done by the force necessary to tow the ship through the given wave environment. He reported reasonable agreement with the experimental measurements,

although only the first order terms were considered, and the ship speed was neglected. There were also several assumptions, namely that the wave and motion amplitudes were small, that the vessel had a fine bow, that the frequency parameter $\omega_e^2/2g$ was of the order of unity and that Fn was of the order of $(B/L)^{½}$.

$$R_{AW} = \frac{\omega_e^3}{2g}(b_z z_a^2 + b_\theta \theta_a^2) \qquad (3)$$

Bhattacharyya (3) discusses Joosen's expression and its derivation, but unfortunately there appear to be several typographical errors in both the expressions and the worked example.

Equation (3) does not allow for the motion of the vessel relative to the wave. If this motion is introduced then the equation becomes:

$$R_{AW} = \frac{\omega_e^3}{2g}(b_z z_a^2 + b_{z+\theta} z_a \theta \cos\varepsilon + b_\theta \theta_a^2) \qquad (4)$$

ω_e is the wave encounter frequency (rad/s)
z_a is the heave amplitude (m)
θ_a is the pitch amplitude (rad)
ε is the difference in phase between heave and pitch
b_z is the heave damping coefficient (kg.s/m)
b_θ is the pitch damping coefficient (kg.s.m)
$b_{z+\theta}$ is the wave damping coefficient (kg.s)

Rearranging this expression to reflect the heave and pitch response amplitude operators (RAOs) gives:

$$R_{AW} = \frac{\omega_e^3}{2g}\left\{\zeta_a^2\left(\frac{z_a}{\zeta_a}\right)^2 b_z - \frac{2\pi\zeta_a^2}{L_W}\left(\frac{z_a}{\zeta_a}\right)\left(\frac{\theta L_W}{2\pi\zeta_a}\right) b_{z+\theta}\cos\varepsilon + \frac{4\pi^2\zeta_a^2}{L_W^2}\left(\frac{\theta_a L_W}{2\pi\zeta_a}\right)^2 b_\theta\right\} \qquad (5)$$

ζ_a is the wave amplitude (m)

Non-dimensionalising this expression in accordance with equation (1) and rearranging gives:

$$\sigma_{AW} = \frac{L\omega_e^3}{2B^2\rho g}\left\{(RAO_Z)^2 b_z - \frac{2\pi}{L_W}(RAO_Z)(RAO_\theta) b_{z+\theta}\cos\varepsilon + \frac{4\pi^2}{L_W^2}(RAO_\theta)^2 b_\theta\right\} \qquad (6)$$

Where RAO_Z is the Heave RAO (z_a/ζ_a)
RAO_θ is the Pitch RAO $(\theta_a L_W/(2\pi\zeta_a))$

For Equation (6) to be useful, it is necessary to be able to estimate the damping coefficients b_z, b_θ, $b_{z+\theta}$. If the hull is split into several adjacent sections throughout the longitudinal extent of the underwater shape, then the damping coefficients can be calculated for each section using charts given in Bhattacharyya (3). Various graphs are presented of the amplitude ratios $\bar{A}$ for two dimensional floating bodies in heaving motion, taken from Grim (4)

$$\bar{A} = \frac{\text{Amplitude of the radiated waves}}{\text{Amplitude of the heaving motion}}$$

$\bar{A}$ is presented as a function of the encounter frequency $\omega_e^2 B_n/(2g)$, for the sectional beam-to-draught ratios B_n/T and for sectional area coefficients β_n . The damping ratios can be calculated for each section and summed through the length to obtain the hull damping coefficients as defined in equations (7), (8) & (9), where ξ is the longitudinal coordinate of the section.

$$b_z = \int b_n d\xi \qquad (7)$$

$$b_{z+\theta} = \int \xi b_n d\xi \qquad (8)$$

$$b_\theta = \int \xi^2 b_n d\xi \qquad (9)$$

The Heave and Pitch RAOs, with their associated phasing information, can be easily obtained from tank tests or from numerical analysis based on strip theory. The damping coefficients can be determined entirely from the geometry as described above. With this information, the additional resistance in waves can be calculated from equation (6)

2.2. Amplitude ratio values

Determining the values of the amplitude ratios $\bar{A}$ from the charts in Bhattacharyya (3) is rather cumbersome and does not permit an entirely numerical solution. Therefore a regression analysis was carried out on data taken from the charts, and the coefficients determined for a fourth order polynomial as a function of $\Omega = \omega_e^2 B_n/(2g)$:

$$\bar{A} = a\,\Omega^4 + b\,\Omega^3 + c\,\Omega^2 + d\,\Omega + e \qquad (10)$$

Values of the coefficients a, b, c, d, and e are given in Tables 3(a) to 3(f) for various sectional areas β_n and beam-to-draught ratios B_n/T.

B_n/T	a	b	c	d	e
0.4	-0.5117	1.9857	-2.9011	1.7521	0.0001
0.8	-0.3831	1.4896	-2.3100	1.8835	-0.0001
1.2	-0.2093	0.9153	-1.6595	1.8187	-0.0008
1.6	-0.2207	0.8954	-1.5260	1.8164	-0.0010
2.0	-0.2720	0.9948	-1.5188	1.8160	-0.0005
2.4	-0.3959	1.3156	-1.7288	1.8642	-0.0004
2.8	-0.4789	1.5295	-1.8715	1.9009	-0.0003
3.6	-0.4853	1.5695	-1.9189	1.9347	0.0001
4.4	-0.4508	1.5027	-1.8990	1.9571	0.0006

Table 3(a): *$\bar{A}$ Coefficients at $\beta_n = 0.5$*

B_n/T	a	b	c	d	e
0.4	-0.4353	1.7190	-2.4699	1.3940	0.0010
0.8	-0.0639	0.5371	-1.3964	1.4786	0.0001
1.2	0.0465	0.0782	-0.8018	1.4479	-0.0008
1.6	0.1509	-0.2155	-0.4985	1.4441	-0.0013
2.0	0.1405	-0.2104	-0.4487	1.4724	-0.0018
2.4	0.0824	-0.0715	-0.5146	1.5041	-0.0017
2.8	0.0562	-0.0112	-0.5326	1.5179	-0.0012
3.6	0.0210	0.0885	-0.5882	1.5411	-0.0007
4.4	0.0063	0.0964	-0.5418	1.5247	-0.0004

Table 3(b): *$\bar{A}$ Coefficients at $\beta_n = 0.6$*

B_n/T	a	b	c	d	e
0.4	-0.3623	1.4897	-2.2231	1.2423	0.0041
0.8	-0.3546	1.4263	-2.2522	1.6117	0.0010
1.2	-0.2372	0.9681	-1.7192	1.6350	0.0018
1.6	-0.1863	0.7947	-1.5064	1.6764	0.0013
2.0	-0.1723	0.7310	-1.4008	1.7104	0.0013
2.4	-0.1530	0.6781	-1.3238	1.7245	0.0013
2.8	-0.2113	0.8274	-1.4123	1.7644	0.0013
3.6	-0.2416	0.9132	-1.4517	1.7965	0.0012
4.4	-0.2357	0.8623	-1.3579	1.7863	0.0014

Table 3(c): *$\bar{A}$ Coefficients at $\beta_n = 0.7$*

B_n/T	a	b	c	d	e
0.4	-0.7119	2.4702	-2.9895	1.3117	0.0028
0.8	-0.5466	2.0506	-2.9121	1.7387	0.0010
1.2	-0.4130	1.5910	-2.4930	1.8506	0.0006
1.6	-0.4445	1.6078	-2.4168	1.9359	0.0007
2.0	-0.3408	1.2819	-2.0806	1.9210	0.0012
2.4	-0.2819	1.0828	-1.8402	1.8940	0.0009
2.8	-0.2328	0.9281	-1.6566	1.8674	0.0009
3.6	-0.1774	0.7463	-1.4220	1.8235	0.0013
4.4	-0.2378	0.8550	-1.4226	1.8237	0.0015

Table 3(d): *$\bar{A}$ Coefficients at $\beta_n = 0.8$*

B_n/T	a	b	c	d	e
0.4	-0.4811	1.8909	-2.4892	1.0726	0.0061
0.8	-0.4096	1.7500	-2.6987	1.5554	0.0029
1.2	-0.4089	1.6090	-2.5121	1.7028	0.0022
1.6	-0.2137	1.0091	-1.9594	1.6941	0.0031
2.0	-0.2045	0.9171	-1.7995	1.7326	0.0032
2.4	-0.2323	0.9494	-1.7627	1.7800	0.0033
2.8	-0.2436	0.9818	-1.7687	1.8275	0.0030
3.6	-0.2263	0.9053	-1.6196	1.8295	0.0029
4.4	-0.1457	0.6696	-1.3796	1.8056	0.0034

Table 3(e): *$\bar{A}$ Coefficients at $\beta_n = 0.9$*

B_n/T	a	b	c	d	e
0.4	-0.6377	2.2621	-2.6322	0.9649	0.0058
0.8	-0.5936	2.3536	-3.2474	1.5489	0.0023
1.2	-0.4405	1.8597	-2.9140	1.7088	0.0029
1.6	-0.3093	1.4120	-2.4956	1.7410	0.0022
2.0	-0.2537	1.1448	-2.1603	1.7450	0.0026
2.4	-0.1978	0.9348	-1.9168	1.7525	0.0020
2.8	-0.1767	0.8293	-1.7622	1.7650	0.0019
3.6	-0.1088	0.5968	-1.4680	1.7547	0.0020
4.4	-0.0804	0.5007	-1.3383	1.7803	0.0015

Table 3(f): *$\bar{A}$ Coefficients at $\beta_n = 1.0$*

2.3. Worked example

The round bilge model described in section 1 was tested in head seas at a full scale speed of 23 knots.

Ship length	L	=	2.190	m
Ship beam	b	=	0.160	m
Draught	T	=	0.086	m
LCB from transom	lcb	=	1.086	m
Speed	U	=	2.174	m/s
Heading	μ	=	180	°
Wave amplitude	ζ_a	=	0.0286	m
SW Density	ρ	=	1025	Kg/m^3

In regular waves with a wavelength λ of 3.18 m;
Wave frequency $\omega_w = (2\pi/\lambda)^{½} = 4.405$ rad/s

Encounter frequency $\omega_e = \omega_w - (\omega_w^2 U/g)\cos\mu$ (11)

$= 4.405 - 4.405^2 \times 2.174/9.81 \times (-1)$
$= 8.705$ rad/s

The recorded motion values at this wave frequency were:
Heave = 61.2 mm
Pitch = 0.0545 rad
Heave phase = -0.576 rad
Pitch phase = -0.105 rad

The motion RAOs are given by:
Heave RAO = 61.2/ 286 = 2.143
Pitch RAO = 0.0545 x 3.18/(2π x 0.0286)
= 0.936

The difference between heave and pitch phase is:
Cos (ε) = cos (-0.576 – (-0.105)) = 0.891

The damping coefficients are now obtained from the hull geometry. The beam at the waterline and the sectional areas are given in Table 4(a). Derived values are given in Table 4(b)

	Distance from transom (m)	**Demihull Beam b_n** (m)	**Sectional Area** (m^2)
1	0.000	0.160	0.0058
2	0.103	0.160	0.0058
3	0.411	0.160	0.0087
4	0.823	0.143	0.0107
5	1.234	0.115	0.0088
6	1.646	0.078	0.0056
7	2.057	0.037	0.0023
8	2.160	0.027	0.0014
9	2.286	0.000	0.0000

Table 4(a): *Breadth at the waterline, and sectional areas*

	Section Area Coefficient β_n	b_n/T	$\omega_e^2\, b_n/2g$
1	0.000	0.160	0.0058
2	0.103	0.160	0.0058
3	0.411	0.160	0.0087
4	0.823	0.143	0.0107
5	1.234	0.115	0.0088
6	1.646	0.078	0.0056
7	2.057	0.037	0.0023
8	2.160	0.027	0.0014
9	2.286	0.000	0.0000

Table 4(b): *Derived values at the sections*

The value of the damping amplitude ration can now be obtained from equation (10), at the values of $\omega_e^2 b_n/2g$, and using the coefficients from Table 3 relating to the required values of β_n and b_n/T from Table 4(b). Interpolation is necessary between the Tables 3(a) to 3(f). This gives values of $\bar{A}$ at the various sections as given in Table 4(c).

The damping coefficients at the sections are obtained from $b_n = \rho g \bar{A}/\omega_e^3$

ξ is the distance of the section from the longitudinal centre of buoyancy *lcb*.

	$\bar{A}$	b_n	ξb_n	$\xi^2 b_n$
1	0.758	8.75	-9.50	10.31
2	0.757	8.74	-8.59	8.44
3	0.683	7.12	-4.80	3.24
4	0.526	4.22	-1.11	0.29
5	0.416	2.63	0.39	0.06
6	0.322	1.58	0.88	0.49
7	0.141	0.30	0.29	0.28
8	0.101	0.15	0.17	0.18
9	0.000	0.00	0.00	0.00

Table 4(c): *Values of $\bar{A}$ and b_n at the sections*

The damping coefficients for the hull are then calculated from equations (7), (8), and (9), using the values from Table 4(c). The trapezoidal rule or the use of Simpson's multipliers if the sections are equally spaced are quite suitable methods for determining the integrals.

These give the following values for the damping coefficients:

$b_z = \int b_n d\xi = 8.38$ kg.s/m

$b_{z+\theta} = \int \xi\, b_n d\xi = -3.67$ kg.s

$b_\theta = \int \xi^2\, b_n d\xi = 3.68$ kg.s.m

All the coefficients in equation (6) have now been calculated, and the value of added resistance can be found for this particular frequency.

f_1 = (Heave RAO)^2 b_z
= 2.143^2 x 8.38 = 38.5 kg.s/m

f_2 = $-2\pi/L_w$(Heave RAO)(Pitch RAO)$b_{z+\theta}$ Cos(ε)
= -2π / 3.18 x 2.143 x 0.936 x (-3.67) x 0.891
= 13.0 kg.s/m

f_3 = $4\pi^2/L_w^2$(Pitch RAO)^2 b_θ
= $4\pi^2$ / 3.18^2 x 0.936^2 x 3.68 = 12.6 kg.s/m

The additional resistance is then given by:

$$\sigma_{AW} = \frac{L\omega_e^3}{2B^2\rho g}(f_1 + f_2 + f_3) \qquad (12)$$

$$\sigma_{AW} = \frac{2.19 \times 8.705^3}{2 \times 0.16^2 \times 1025 \times 9.807}(38.5 + 13.0 + 12.6)$$

σ_{AW} = 2.807 x 64.1 = 179.8

Applying equation (1) gives the value of added resistance:

R_{AW} = 179.8 x 1025 x $.0286^2$ x (0.16^2/2.19) x g

R_{AW} = 18.8 N

3. COMPARISON OF RESULTS

3.1 Comparison of experiment and numerical method

The worked example in 2.3 above is an example at one wave frequency. The same calculation has to be carried out over a range of wave frequencies in order to obtain some useful result that can be applied to a craft in operation.

The results of such a calculation are compared with the model test results in Table 5 and Figure 4.

ω_e (rad/s)	R_{AW} Model tests (N)	R_{AW} Calculation (N)	$\frac{\omega_e^2}{2g}$
4.237	0.00	0.40	0.92
5.269	2.13	1.00	1.42
5.960	1.97	2.00	1.81
6.870	5.27	5.50	2.41
7.345	9.34	8.30	2.75
8.066	17.65	16.30	3.32
8.723	20.29	18.80	3.88
9.442	17.13	11.60	4.55
11.66	7.26	2.30	6.94

Table 5: *Comparison of Added Resistance from model tests and from calculation*

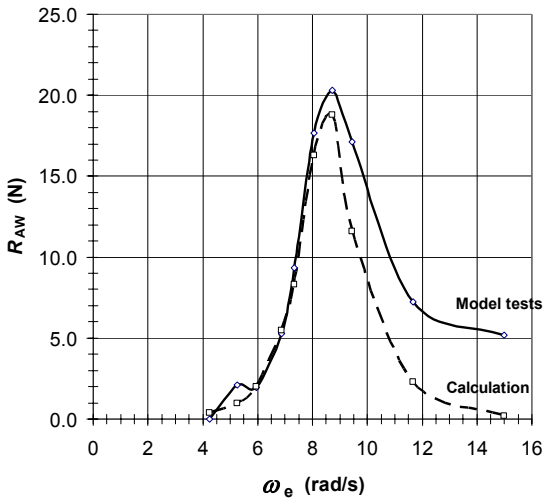

Figure 4: *Comparison of model tests and numerical calculation*

The calculation agrees well with the model test results at the lower wave encounter frequencies. It accurately reflects the magnitude and frequency of the peak in the curve, but under-predicts the magnitude of added resistance at frequencies higher than the hump frequency. This is hardly surprising, as the theory is valid only for values of $\omega_e^2/2g$ of around unity, and as can be seen from the values of this parameter given in Table 5, at the higher encounter frequencies the value becomes much greater than unity.

3.2 Added resistance at other headings

The experiments were carried out in head seas and following seas. The presented numerical method has been presented for head seas only. It might be considered as reasonable to apply the numerical method to other headings, where the encounter frequency is modified by the inclusion of the cos(μ) term. However, it should be noted that the method does not include for the roll motion of the vessel, which at headings other than head seas and following seas will be a factor in the overall additional resistance. For a catamaran operating in "normal" sea states it has been observed that the vessel speed is not affected unduly by rolling in beam seas. The inference is that the additional resistance owing to rolling may be a lesser magnitude than that due to heaving and pitching. For a catamaran of course there is no true "rolling" motion, as unlike a monohull the hull does not rotate about a longitudinal access, rather one demihull heaves out of phase with the other demihull.

If the rolling motion of the catamaran is ignored, then the numerical method should be valid for other headings as long as the correct heave and Pitch RAOs are utilized for that particular heading.

It is possible for the round bilge hull form at high speed to obtain some broad idea of the added resistance at all headings based upon the tank test results in head seas and following seas. For example at a wave frequency of 0.70 rad/s, the non-dimensional added resistance in head seas has a value of 0.0095, and in stern seas it has a value of -0.001. These two points, illustrated in Figure 5, do not allow any conclusion to be drawn at other headings.

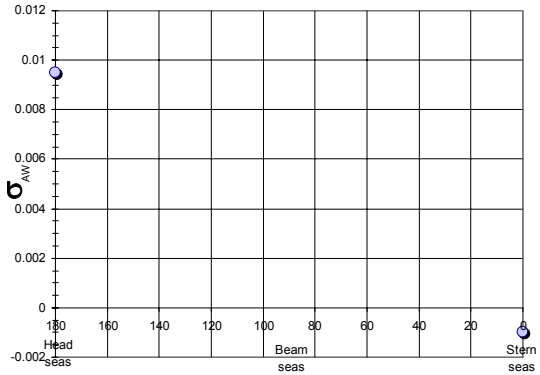

Figure 5: *Added resistance in head seas and following seas, round bilge hull form at 32.2 knots*

It is noted that at a certain heading angle in following seas the apparent speed of the wave relative to the vessel may be zero. For a vessel traveling at 32.2 knots, and in a regular sea with a wave frequency of 0.9 rad/s, the encounter frequency becomes zero at a heading of 49 degrees, based upon the relationship given in Equation (11). Including the additional data point where a heading of 49° gives zero added resistance, then a broad relationship between heading and additional resistance may be drawn, as illustrated in Figure 6.

It must be noted that this approach can only be valid for small wave heights, as at large wave heights and wave lengths similar to the craft length or longer, the vessel would tend to surf down the wave face and travel at the speed of the wave with an apparently greatly reduced resistance.

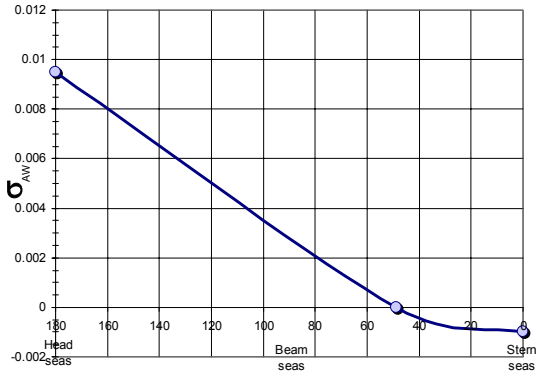

Figure 6: *Added resistance in head seas and following seas, round bilge hull form at 32.2 knots*

CONCLUSIONS

Experimental measurements of added resistance on a small model have been successfully conducted for two types of hull form, representative of commercial hull forms currently in use.

The values of additional resistance in following seas are less accurately represented, owing to the limitations imposed by the towing tank length and the resultant small number of encountered waves.

It is clearly demonstrated for these two models that the additional resistance for the hard chine hull form is considerably greater than that of the round bilge hull form, despite the considerably greater beam of the round bilge hull form.

The numerical method shows good agreement with the experimental method, particularly at the lower encountered wave frequency values. At higher frequencies the limitations of the method become evident and the accuracy falls off. The peak of added resistance against wave frequency is clearly defined, and is related to the ship motion characteristics.

A regression analysis was carried out to define the values of the damping coefficients in heave, from published charts of the wave amplitude ratios.

Although presented for catamarans, the same numerical approach would be valid for monohulls, however, the limitations of the theory, particularly the speed relationship, may be compromised by the additional beam of a monohull, and it is likely that the method would be less accurate than it appears to be for a catamaran.

ACKNOWLEDGMENTS

The authors wish to thank *AUSTAL Ships* for their support in allowing this paper to be presented. The hull forms described in the paper are typical of those used in commercial ferries, but are not necessarily representative of *AUSTAL* hull forms.

REFERENCES

1. Havelock T.H., 1958, "The effect of Speed of Advance upon Damping of Heave and Pitch", *Trans.RINA*, , **86**, pp. 1-14.

2. Joosen W.P.A., 1966, "Added Resistance of Ships in Waves", *Proc. 6th ONR Symposium on Naval Hydrodynamics,* Washington DC, USA, pp12.

3. Bhattacharyya R., 1978, "Dynamics of Marine Vehicles", *Ocean Engineering*, John Wiley and Sons, New York, USA.

4. Grim O., 1959, "Die Schwingungen von Schwimmenden, Zwei-dimensionalen Körpern", *HSVA Report 1171*, Germany

5. Lamb G.R., MacGregor J.R, & Holcomb R.S., May 1991, "Ferry Routes, Ship Motions and Passenger Comfort – analyzing the relationship ", Cruise and Ferry 91 Conference, Olympia, London.

6. Lloyd A.R.J.M., 1998, "Seakeeping – Ship Behaviour in Rough Weather", *published by the Author*, available through RINA, London